Cancer Research

Bcl9/Bcl9l Are Critical for Wnt-Mediated Regulation of Stem Cell Traits in Colon Epithelium and Adenocarcinomas

Jürgen Deka[1,2], Norbert Wiedemann[1], Pascale Anderle[4], Fabienne Murphy-Seiler[1], Jennyfer Bultinck[1], Sven Eyckerman[1], Jean-Christophe Stehle[3], Sylvie André[1], Nathalie Vilain[1], Olav Zilian[1], Sylvie Robine[5], Mauro Delorenzi[6], Konrad Basler[7], and Michel Aguet[1,2]

Abstract

Canonical Wnt signaling plays a critical role in stem cell maintenance in epithelial homeostasis and carcinogenesis. Here, we show that in the mouse this role is critically mediated by Bcl9/Bcl9l, the mammalian homologues of Legless, which in *Drosophila* is required for Armadillo/β-catenin signaling. Conditional ablation of Bcl9/Bcl9l in the intestinal epithelium, where the essential role of Wnt signaling in epithelial homeostasis and stem cell maintenance is well documented, resulted in decreased expression of intestinal stem cell markers and impaired regeneration of ulcerated colon epithelium. Adenocarcinomas with aberrant Wnt signaling arose with similar incidence in wild-type and mutant mice. However, transcriptional profiles were vastly different: Whereas wild-type tumors displayed characteristics of epithelial-mesenchymal transition (EMT) and stem cell–like properties, these properties were largely abrogated in mutant tumors. These findings reveal an essential role for Bcl9/Bcl9l in regulating a subset of Wnt target genes involved in controlling EMT and stem cell–related features and suggest that targeting the Bcl9/Bcl9l arm of Wnt signaling in Wnt-activated cancers might attenuate these traits, which are associated with tumor invasion, metastasis, and resistance to therapy. *Cancer Res; 70(16); 6619–28. ©2010 AACR.*

Introduction

Canonical Wnt signaling regulates critical processes during embryonic development and adult tissue renewal, and aberrant activation of this pathway is associated with colorectal cancer and other cancers (1). Wnt-induced transcriptional regulation is mediated through a complex of Lef1/Tcf transcription factors and stabilized β-catenin that interacts with numerous cofactors (2). This complex includes Legless (Lgs; ref. 3), which tethers Pygopus to the most NH_2-terminal repeat of Armadillo (Arm)/β-catenin and in *Drosophila* is required for the transcriptional activity of the complex (3, 4). In mammalian cells, BCL9 proteins contribute to, but may not be obligatory for, β-catenin–mediated transcription (5, 6). BCL9L mRNA knockdown in a human colon cancer cell line induced an epithelial phenotype that was associated with the translocation of β-catenin from the nucleus to the cell membrane, suggesting that BCL9L might regulate the switch between the adhesive and transcriptional functions of β-catenin (5). BCL9L upregulation has been associated with breast (7) and colon cancers (8–10), and BCL9 has recently been reported to enhance β-catenin–mediated transcription and increase the proliferation as well as the metastatic potential of tumor cells (9).

To investigate the role of Bcl9 proteins in mice, we generated loxP alleles of the murine lgs orthologues, *Bcl9* and *Bcl9l*, which were crossed into transgenic strains expressing Cre recombinase either constitutively or inducibly under the control of the villin promoter (11). Thereby, deletion of *Bcl9* and *Bcl9l* was targeted selectively to the intestinal epithelium, for which the essential role of Wnt signaling for epithelial homeostasis is well documented (12).

Here, we report that ablation of Bcl9/Bcl9l in the intestinal epithelium selectively abrogated the expression of a subset of Wnt-regulated genes, which are critical for controlling stem cell–like properties, both in normal colon epithelium and in a colon adenocarcinoma model.

Materials and Methods

Generation of *Bcl9*$^{-/-}$/*Bcl9l*$^{-/-}$ mice

For the generation of conditional *Bcl9*$^{-/-}$/*Bcl9l*$^{-/-}$ mice, exon V of *Bcl9* and exons VI and VII of *Bcl9l* were flanked with loxP sites in adjacent introns. Simultaneous deletion of both

Authors' Affiliations: [1]Swiss Institute for Experimental Cancer Research (ISREC), [2]Swiss National Center of Competence in Research Molecular Oncology, School of Life Sciences, Ecole Polytechnique Fédérale de Lausanne (EPFL); [3]Division of Experimental Pathology, Institut Universitaire de Pathologie, Lausanne, Switzerland; [4]Laboratory of Experimental Oncology, Oncology Institute of Southern Switzerland (IOSI), Bellinzona, Switzerland; [5]Morphogenesis and Intracellular Signaling, Institut Curie-Centre National de la Recherche Scientifique, Paris, France; [6]Swiss Institute of Bioinformatics (SIB) and Faculty of Biology and Medicine of University Lausanne, Lausanne-Dorigny, Switzerland; and [7]Institut für Molekularbiologie, Universität Zürich, Zürich, Switzerland

Note: Supplementary data for this article are available at Cancer Research Online (http://cancerres.aacrjournals.org/).

J. Deka and N. Wiedemann are co-first authors.

Corresponding Author: Michel Aguet, Ecole Polytechnique Fédérale de Lausanne (EPFL), Rue du Bugnon 25, Lausanne 1011, Switzerland. Phone: 41-21-314-7217; Fax: 41-21-314-7115; E-mail: michel.aguet@epfl.ch.

doi: 10.1158/0008-5472.CAN-10-0148

genes in the intestinal epithelium was achieved by crossing with *villin-Cre-ER^{T2}* or *villin-Cre* transgenic mice, resulting in *vil-Cre-ER^{T2}-Bcl9$^{loxP/loxP}$/Bcl9l$^{loxP/loxP}$* (on tamoxifen induction: *vil-Cre-ER^{T2}-Bcl9$^{-/-}$/Bcl9l$^{-/-}$*) and *vil-Cre-Bcl9$^{-/-}$/Bcl9l$^{-/-}$* lines. More detailed information is available in Supplementary Materials and Methods.

Mouse experimentation

Mouse experiments were performed in accordance with Swiss guidelines and approved by the Veterinarian Office of Vaud, Switzerland. The protocols for gene ablation in *vil-Cre-ER^{T2}-Bcl9$^{loxP/loxP}$/Bcl9l$^{loxP/loxP}$* mice and the induction of ulcerative colitis and colon chemical carcinogenesis are provided in Supplementary Materials and Methods.

Laser dissection microscopy

Samples of colon tissue were washed in chilled PBS, embedded in optimal cutting temperature compound, and frozen immediately. Frozen sections (14 μm) were mounted on Leica membranes (Leica Microsystems) for laser dissection microscopy, fixed in ethanol, and colored with Mayer's hematoxylin. Membranes were rinsed in water and ethanol and air-dried. Samples were prepared using a laser-dissecting microscope (MMI-Nikon, Leica Microsystems). Total RNA (20 μL) was extracted using the PicoPure RNA Isolation Kit (MDS Analytical Technologies).

Comparative gene expression analysis

RNA quality was assessed using the Agilent 2100 Bioanalyzer (Agilent Biotechnologies) and RNA was quantified with a NanoDrop spectrophotometer (Witec AG). Total RNA (30 ng) was amplified using the NuGEN WT-Ovation Pico kit and the cDNA was hybridized to Affymetrix Mouse Genome 430 2.0 arrays. Robust multiarray averaging and quantile normalization were used to quantify gene expression (R, Bioconductor, RMA package). Significant differences were identified by applying a moderated *t* test approach (R, Bioconductor, LIMMA package; ref. 13). The gene expression microarray data reported herein were deposited in the Gene Expression Omnibus repository (accession no. GSE21603; see Supplementary Data for details). If not indicated otherwise, a threshold of an adjusted $P \leq 0.05$ (Benjamini-Hochberg FDR correction) was used to identify significant changes between wild-type and mutant samples.

Genes with significantly different expression in wild-type as compared with *Bcl9$^{-/-}$/Bcl9l$^{-/-}$* tumors were analyzed with the functional annotation chart tool in DAVID (14). Gene ontology (GO) terms related to "biological processes" were used. Fisher's exact test was applied to calculate significance. Terms with an adjusted $P < 0.05$ (Benjamini-Hochberg FDR correction) were defined as significant.

Gene set enrichment analysis (GSEA) was carried out according to Subramanian and colleagues (15). *P* values were computed using a bootstrap distribution created by resampling gene sets of the same cardinality. This is a heuristic approach to identifying gene sets and biological functions that, given the samples used, seem to be most related to the observed effects. Its *P* values could overestimate the appropriate level of confidence in relation to the extent of the biological variability that was sampled and are better considered as comparative scores between gene sets. Lists of direct Wnt targets ($n = 24$), genes involved in epithelial-mesenchymal transition (EMT; $n = 13$), and genes enriched in intestinal stem cells marked by the expression of Lgr5 were generated manually (Fig. 4A). Heat maps were generated using Cluster 3.0 and TreeView (ref. 16; http://rana.lbl.gov/EisenSoftware.htm). As a similarity measurement and clustering method, centered correlation and average linkage clustering, respectively, were applied. The Davies-Bouldin index was determined as described (17), whereby intercluster and intracluster differences were calculated using the average of all pairwise comparisons. The Davies-Bouldin index is a ratio that compares the average distance within a group of samples to that between groups. A value of 2 indicates no difference and smaller values indicate better discrimination with a theoretical minimum of 0. All configurations tested were obtained by cutting the hierarchical tree into two clusters that always corresponded to the five mutant and the five wild-type samples.

The significance of quantitative real-time PCR (qRT-PCR) data was determined using Student's *t* test ($P \leq 0.05$).

Standard protocols and reagents

Quantitative RT-PCR, *in situ* hybridization, and immunohistochemistry were carried out according to standard protocols. Details and reagents are provided in Supplementary Materials and Methods.

Results

Ablation of Bcl9/Bcl9l results in decreased intestinal stem cell marker expression and impaired epithelial regeneration

Despite the rather low overall sequence identity, mouse Bcl9 and Bcl9l share seven highly conserved domains (18), suggesting that they might be functionally redundant. As both genes were expressed in the small intestine and colon, with Bcl9 generally expressed at an approximately 2- to 4-fold higher level than Bcl9l (data not shown), all loss-of-function experiments presented herein were carried out on a compound *Bcl9/Bcl9l* mutant background. Conditional loss-of-function alleles of *Bcl9* and *Bcl9l* (GenBank accession nos. AY296061 and AY296058) were generated by flanking exons encoding the functionally essential β-catenin interaction domain with loxP sites (Supplementary Fig. S1A). Mouse strains with compound inducible or constitutive deletion of both genes confined to the intestinal epithelium were obtained through crossing with *villin-Cre-ER^{T2}* or *villin-Cre* transgenic mice, respectively (11), resulting in *vil-Cre-ER^{T2}-Bcl9$^{loxP/loxP}$/Bcl9l$^{loxP/loxP}$* (on tamoxifen induction: *vil-Cre-ER^{T2}-Bcl9$^{-/-}$/Bcl9l$^{-/-}$*) and *vil-Cre-Bcl9$^{-/-}$/Bcl9l$^{-/-}$* lines. Unless stated otherwise, experiments reported herein were carried out initially on a *villin-Cre-ER^{T2}* background and reproduced using the constitutive *villin-Cre* transgene. *Bcl9$^{loxP/loxP}$/Bcl9l$^{loxP/loxP}$* littermates lacking the *Cre* transgene served as controls.

Deletion of *Bcl9/Bcl9l* proved highly efficient in both strains (Supplementary Fig. S1B–D). Induced ablation of Bcl9/Bcl9l in the *villin-Cre-ER^{T2}* strain assessed 23 weeks after tamoxifen administration proved similarly efficient as in mice with constitutively active Cre, suggesting that the deletion was unaffected by epithelial renewal and therefore had encompassed the epithelial progenitor cell compartment.

Neither induced nor constitutive ablation of Bcl9/Bcl9l in the intestinal epithelium resulted in any overt anomalies, and all intestine-specific cell lineages were equally present in mutant and control mice (Supplementary Fig. S2).

Canonical Wnt signaling as revealed by expression of the direct target gene *Axin2* (19) did not seem to be significantly altered in small intestinal epithelium and was only mildly reduced in the colon epithelium of mutant mice (Supplementary Fig. S1D). To assess Wnt signaling more comprehensively, EDTA-dissociated colon epithelial cells (20) from three pools each of wild-type and *Bcl9/Bcl9l*–mutant mice were subjected to an exploratory comparative gene expression profiling. Using an adjusted $P < 0.05$ as a threshold (see Materials and Methods), no significant gene expression changes were observed between wild-type and mutant colon epithelium. Notably, Wnt target gene expression (http://www.stanford.edu/~rnusse/wntwindow.html) did not prove to be significantly affected in *Bcl9/Bcl9l*–mutant colon epithelium, strikingly, with the exception of the intestinal stem cell marker Lgr5 (21), which was reduced 3.4-fold (P = 2E–5, not adjusted for multiple testing). A GSEA (15) was therefore carried out with a recently reported set of genes with ≥2-fold enriched expression in Lgr5-positive stem cells isolated from the small intestine (22); results revealed a weak but significant enrichment in wild-type versus *Bcl9/Bcl9l*–mutant colon epithelium (P = 0.019). The expression of genes enriched in this analysis was further assessed by qRT-PCR (Fig. 1A). Expression of the other genes coexpressed selectively in Lgr5-positive small intestine stem cells was significantly

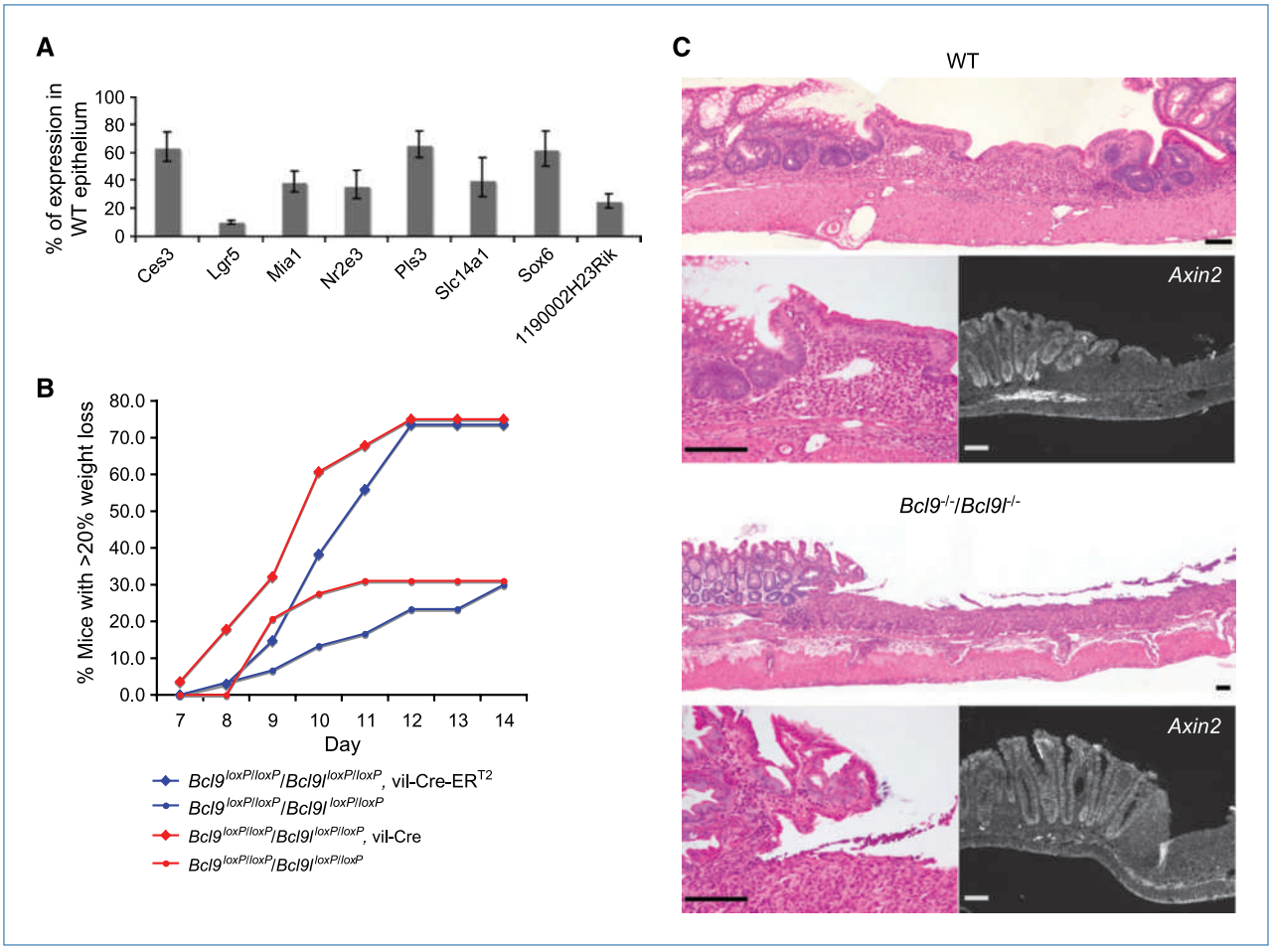

Figure 1. Reduced intestinal stem cell marker expression and impaired regeneration of *Bcl9$^{-/-}$/Bcl9l$^{-/-}$* epithelium. A, quantification by qRT-PCR in colon epithelium of genes with enriched expression in small intestine stem cells (22). Only genes with significantly reduced expression in *Bcl9$^{-/-}$/Bcl9l$^{-/-}$* compared with wild-type epithelium are shown (n = 7 ± SE for wild-type epithelium; n = 6 ± SE for *Bcl9$^{-/-}$/Bcl9l$^{-/-}$* epithelium; $P \leq 0.05$). B, percentages of wild-type and *Bcl9$^{-/-}$/Bcl9l$^{-/-}$* mice with >20% weight loss after treatment with DSS (n = 30, P = 0.00095 for *vil-Cre-ERT2-Bcl9$^{-/-}$/Bcl9l$^{-/-}$* mice; n = 28, P = 0.00136 for *vil-Cre-Bcl9$^{-/-}$/Bcl9l$^{-/-}$* mice). C, H&E staining and analysis of *Axin2* expression by *in situ* hybridization on sections of mouse colon showing representative DSS-induced lesions 6 d after DSS administration was terminated. Bar, 150 μm.

diminished in the absence of Bcl9/Bcl9l. Interestingly, expression of achaete scute-like 2 (Ascl2), which has recently been reported to control intestinal stem cell fate (22), did not prove to be significantly different between wild-type and mutant colon epithelium (Supplementary Fig. S4).

To investigate the regenerative capacity of *Bcl9*$^{-/-}$/*Bcl9l*$^{-/-}$ intestinal epithelium, mice were challenged by p.o. administration for 7 days of the irritant dextran sulfate sodium (DSS), which has been described to provoke severe colitis with extensive ulcerations (23). Animals were monitored for weight loss and sacrificed when the loss reached 20% (Fig. 1B). Whereas the majority of control mice recovered 5 to 7 days after DSS administration was discontinued and had lost less than 20% body weight, the majority of mutant mice crossed the 20% weight loss percentile. At this stage, mutant mice showed considerably more extended ulcerative lesions within the colon epithelium. Whereas control lesions underwent visible re-epithelialization with the formation of new crypts at wound borders, the large open wounds of mutant mice displayed no evidence of ongoing epithelial regeneration (Fig. 1C). Like in mutant colon epithelium, *Axin2* expression seemed slightly reduced at mutant wound borders, this difference did not prove to be significant, however, when quantified by qRT-PCR (data not shown). Thus, ablation of Bcl9/Bcl9l resulted in reduced expression of intestinal stem cell markers in *Bcl9/Bcl9l*–mutant colon epithelium and was associated with impaired epithelial regeneration capacity.

Bcl9$^{-/-}$/*Bcl9l*$^{-/-}$ adenocarcinomas show impaired expression of selected Wnt target genes

To investigate the effect of Bcl9/Bcl9l ablation on tumorigenesis, 6- to 8-week-old mice were exposed first to a single dose of dimethylhydrazine, which is metabolized in the liver to carcinogenic azoxymethane, followed by 7 days of p.o. administration of DSS in the drinking water. This regimen results in the emergence of dysplastic adenomas, which progress to differentiated adenocarcinomas that are morphologically similar to human colorectal adenocarcinoma and typically harbor β-catenin–stabilizing mutations of glycogen synthase kinase-3β phosphorylation sites (24). Accordingly, these tumors presented hallmarks of active Wnt signaling such as accumulation of nuclear β-catenin and expression of Wnt target genes (Fig. 2).

Vil-Cre-ER^{T2}-*Bcl9*$^{-/-}$/*Bcl9l*$^{-/-}$ and *vil-Cre-Bcl9*$^{-/-}$/*Bcl9l*$^{-/-}$ mice developed tumors in the distal colon at a slightly higher frequency than their littermate controls (not reproducibly significant; Fig. 2A). Tumors from mutant mice were generally of smaller size (mean tumor diameter: wild-type tumors, 4.4 ± 1.7 mm, $n = 58$; *Bcl9*$^{-/-}$/*Bcl9l*$^{-/-}$ tumors, 2.4 ± 1.0 mm, $n = 110$; two-sample t test $P = 5.1E{-}12$). Bromodeoxyuridine incorporation, however, did not prove to be significantly different (data not shown). To rule out that tumors emerged from residual wild-type epithelial cells in otherwise mutant epithelium, cDNA was obtained from laser capture microdissected tumor samples, and expression of wild-type *Bcl9* and *Bcl9l* transcripts assessed by qRT-PCR (Fig. 2B). The residual level of wild-type transcripts in tumors from mutant mice was incompatible with heterozygous escaper tumor cells and likely due to stromal components. Wild-type and mutant tumors presented as exophytic, low-grade adenocarcinomas (Fig. 2C) and were indistinguishable on H&E staining.

Nuclear accumulation of β-catenin was indicative of Wnt pathway activation and expression of *Axin2* provided evidence for Wnt signaling activity, both in wild-type and mutant tumors, whereby *Axin2* expression seemed to be reduced in the absence of Bcl9/Bcl9l (Fig. 2C).

To assess at a genome-wide level to what extent loss of Bcl9/Bcl9l function affected gene expression, individual cRNA probes were prepared from microdissected tumor epithelium of five randomly chosen tumors (two wild-type and three *vil-Cre-Bcl9*$^{-/-}$/*Bcl9l*$^{-/-}$ littermates) and subjected to comparative gene expression profiling. Despite the close morphologic resemblance, transcriptomes from *Bcl9*$^{-/-}$/*Bcl9l*$^{-/-}$ tumors proved vastly different from wild-type tumors.

Unsupervised hierarchical clustering with all probe sets formed two well-separated clusters according to the genotypes (Fig. 3A). Based on adjusted $P \leq 0.05$ as a threshold (see Materials and Methods), 746 genes were expressed at a higher level and 946 at a lower level in wild-type than in *Bcl9*$^{-/-}$/*Bcl9l*$^{-/-}$ tumors (Supplementary Table S1). Analysis of GO terms contained within the domain "biological processes" (14) sorted according to their overrepresentation ($P < 0.05$) revealed a marked enrichment in wild-type tumors of processes relating to development (Supplementary Table S2). GO terms relating to Wnt signaling were the only pathway-associated terms enriched in wild-type samples. In *Bcl9*$^{-/-}$/*Bcl9l*$^{-/-}$ tumor samples, GO terms related to immune response were predominantly enriched (Supplementary Table S2), mainly due to the higher expression of epithelial chemokines and genes expressed in T and B cells (Supplementary Table S1). Preliminary evidence obtained from microdissected normal colon epithelium indicated that expression of chemoattractants in mutant tumor samples was closer to that of wild-type or mutant epithelium than to that of wild-type tumors (data not shown).

To assess to what extent canonical Wnt signaling was affected in *Bcl9/Bcl9l*–mutant tumors, a set of 24 Wnt target genes relevant to human colon and/or other cancers, with a proven direct transcriptional control through TCF binding sites, was assembled from the Wnt home page and published reports [http://www.stanford.edu/~rnusse/wntwindow.html; *Apcdd1* (ref. 25), *Prox1* (ref. 26), *Vim* (ref. 27), *S100a4* (ref. 28), *Fscn1* (ref. 29), and *T* (ref. 30)]. This set was used for hierarchical clustering and GSEA (Fig. 3B) and revealed a significantly enriched expression in wild-type compared with *Bcl9*$^{-/-}$/*Bcl9l*$^{-/-}$ tumors ($P = 4.3E{-}05$). Accordingly, intercluster separation assessed by the Davies-Bouldin index (17) proved stronger with this 24 Wnt target gene set than with the set of the 24 genes varying the most across all samples. These data unequivocally showed the relatedness of Bcl9/Bcl9l to the Wnt pathway. A subset of the Wnt target genes was downregulated in *Bcl9*$^{-/-}$/*Bcl9l*$^{-/-}$ tumors as compared with wild-type tumors (Fig. 3B). The expression of all 24 genes contained in the Wnt target gene set was verified by qRT-PCR (Fig. 3C).

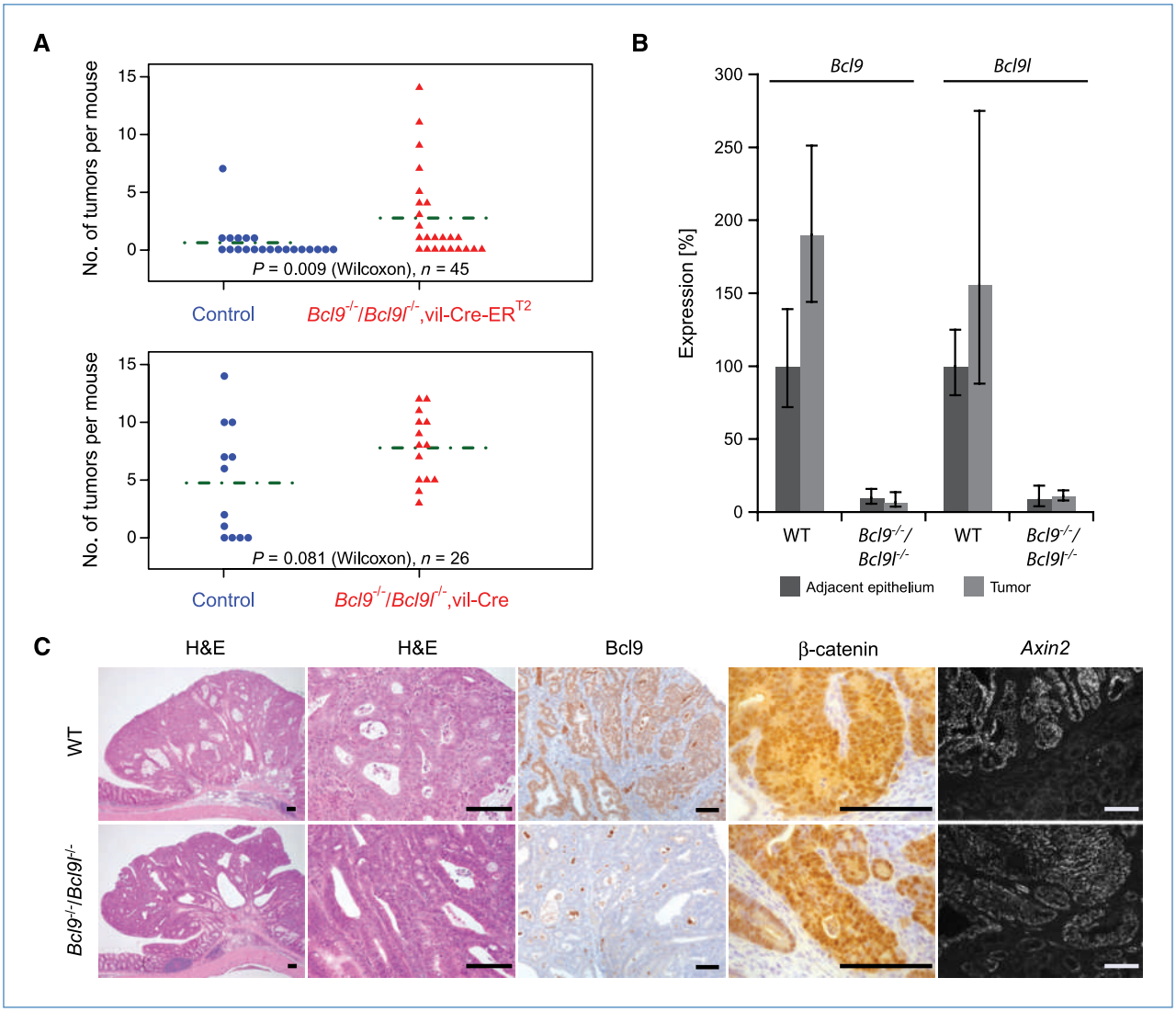

Figure 2. *Bcl9*$^{-/-}$/*Bcl9l*$^{-/-}$ mice develop colon tumors with hallmarks of active Wnt signaling. A, number of tumors that developed in *Bcl9*$^{-/-}$/*Bcl9l*$^{-/-}$ mice and littermate controls. Results from two independent experiments are shown that were carried out with either *vil-Cre-ERT2- Bcl9*$^{-/-}$/*Bcl9l*$^{-/-}$ or *vil-Cre- Bcl9*$^{-/-}$/*Bcl9l*$^{-/-}$ mice. Mice were sacrificed 20 or 25 wk, respectively, after exposure to dimethylhydrazine. B, *Bcl9* and *Bcl9l* transcript levels in dimethylhydrazine/DSS–induced colon tumors and adjacent normal colon epithelium were determined by qRT-PCR using total RNA extracted from microdissected tumor tissue (nontumorous epithelium, $n = 5 \pm$ SE; wild-type tumor tissue, $n = 3 \pm$ SE; mutant tumor tissue, $n = 8 \pm$ SE). Expression levels in normal epithelium were set to 100%. C, tumor morphology and expression of Bcl9 and the Wnt signaling markers β-catenin and *Axin2*. Bars, 150 μm.

Bcl9$^{-/-}$/*Bcl9l*$^{-/-}$ adenocarcinomas show reduced expression of EMT and stem cell–associated markers

The subset of Wnt target genes with reduced expression in *Bcl9*$^{-/-}$/*Bcl9l*$^{-/-}$ tumors included genes relating to mesenchymal phenotypes [*vimentin* (31); *T* (*brachyury*; ref. 30)]. To address to what extent the processes relating to EMT, known to be mediated in part by Wnt signaling (32), were more generally affected in the absence of Bcl9/Bcl9l, a set of 13 genes described to relate to EMT was assembled (32, 33). Clustering the tumor samples with this set revealed a stronger separation between the two genotype clusters than using the 13 genes varying the most across all samples (Fig. 3B). Verification by qRT-PCR confirmed that a number of EMT-inducing transcription factors present in wild-type tumors were in part strongly downregulated in *Bcl9*$^{-/-}$/*Bcl9l*$^{-/-}$ tumors, consistent with the marked reduction of the mesenchymal marker proteins vimentin, T (brachyury), and fibronectin 1 (Fig. 3C).

Recent evidence suggests that EMT may be associated with the induction of stem cell–like properties (32, 34). A GSEA was therefore carried out with the same set of 50 genes with ≥2-fold enriched expression in Lgr5-positive intestinal stem cells that was previously used to probe the transcriptomes of wild-type and *Bcl9*$^{-/-}$/*Bcl9l*$^{-/-}$ colon epithelium (ref. 22; Fig. 1A). This analysis revealed a highly significant enrichment for expression of this gene set in the wild-type

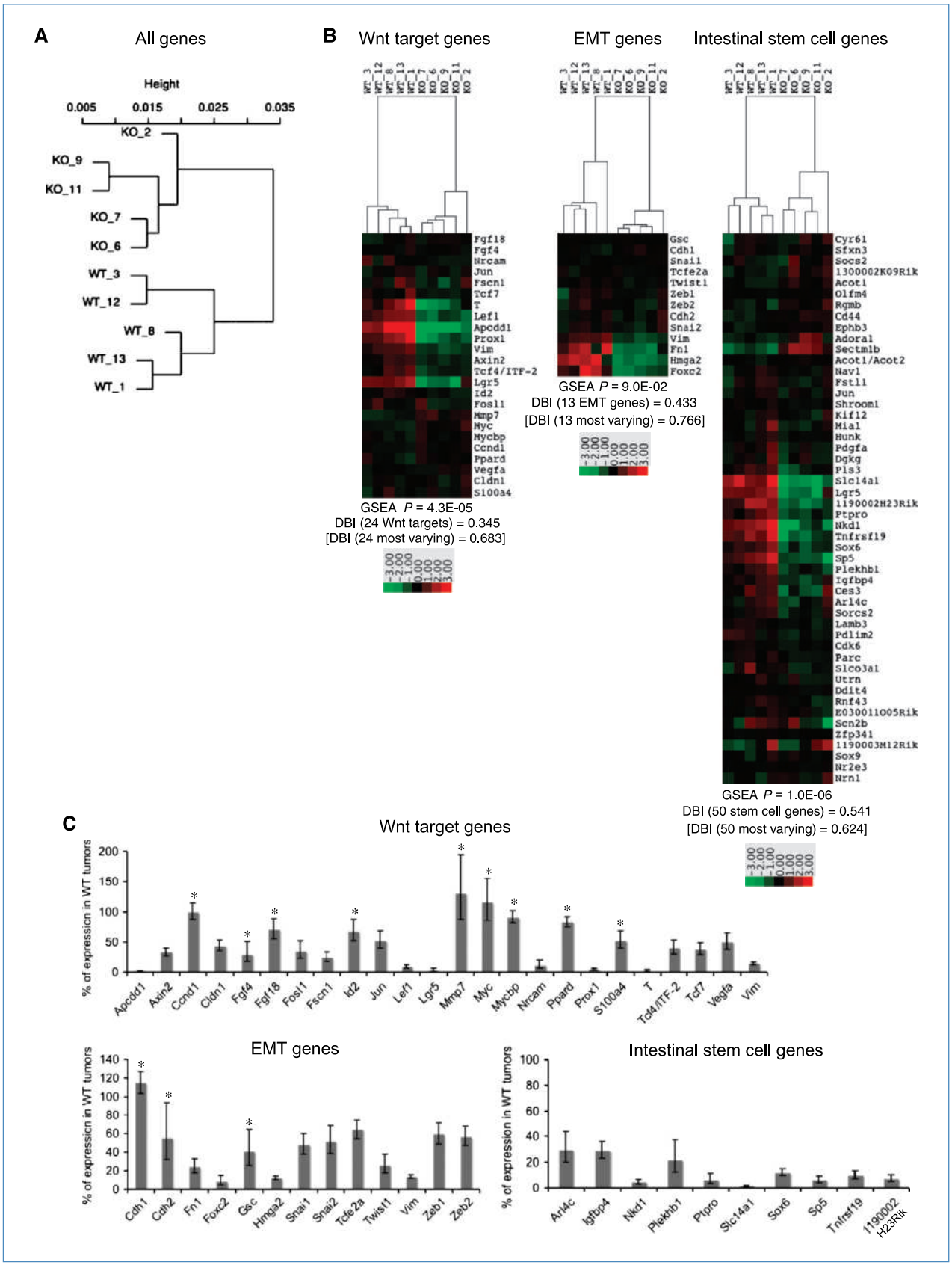
A
All genes
Height
0.005
0.015
0.025
0.035
KO_2
KO_9
KO_11
KO_7
KO_6
WT_3
WT_12
WT_8
WT_13
WT_1
B
Wnt target genes
EMT genes
Intestinal stem cell genes
Fgf18
Fgf4
Nrcam
Jun
Fscn1
Tcf7
T
Lef1
Apcdd1
Prox1
Vim
Axin2
Tcf4/ITF-2
Lgr5
Id2
Fosl1
Mmp7
Myc
Mycbp
Ccnd1
Ppard
Vegfa
Cldn1
S100a4
GSEA P = 4.3E-05
DBI (24 Wnt targets) = 0.345
[DBI (24 most varying) = 0.683]
Gsc
Cdh1
Snai1
Tcfe2a
Twist1
Zeb1
Zeb2
Cdh2
Snai2
Vim
Fn1
Hmga2
Foxc2
GSEA P = 9.0E-02
DBI (13 EMT genes) = 0.433
[DBI (13 most varying) = 0.766]
Cyr61
Sfxn3
Socs2
1300002K09Rik
Acot1
Olfm4
Rgmb
Cd44
Ephb3
Adora1
Sectm1b
Acot1/Acot2
Nav1
Fstl1
Jun
Shroom1
Kif12
Mia1
Hunk
Pdgfa
Dgkg
Pls3
Slc14a1
Lgr5
1190002H23Rik
Ptpro
Nkd1
Tnfrsf19
Sox6
Sp5
Plekhb1
Igfbp4
Ces3
Arl4c
Sorcs2
Lamb3
Pdlim2
Cdk6
Parc
Slco3a1
Utrn
Ddit4
Rnf43
E030011O05Rik
Scn2b
Zfp341
1190003M12Rik
Sox9
Nr2e3
Nrn1
GSEA P = 1.0E-06
DBI (50 stem cell genes) = 0.541
[DBI (50 most varying) = 0.624]
C
Wnt target genes
% of expression in WT tumors
EMT genes
Intestinal stem cell genes
Cdh1
Cdh2
Fn1
Foxc2
Gsc
Hmga2
Snai1
Snai2
Tcfe2a
Twist1
Vim
Zeb1
Zeb2
Ari4c
Igfbp4
Nkd1
Plekhb1
Ptpro
Slc14a1
Sox6
Sp5
Tnfrsf19
1190002H23Rik

tumor samples (P = 1E−6), and accordingly, intercluster separation was superior to the separation observed with the control set of 50 genes varying the most across all samples (Fig. 3B). Expression of genes contained in this stem cell–associated gene set that were ≥2-fold decreased in mutant tumors was validated by qRT-PCR (Fig. 3C).

For selected genes, expression differences between wild-type and *Bcl9*$^{-/-}$/*Bcl9l*$^{-/-}$ tumor samples were confirmed by immunohistochemistry. Vimentin, whose expression can be directly regulated by β-catenin/Tcf (27), is one of the most reliable mesenchymal markers. The difference in vimentin expression in wild-type compared with *Bcl9*$^{-/-}$/*Bcl9l*$^{-/-}$ tumors, however, was clearly attributed to its loss in mutant epithelial cells (Fig. 4A, c versus d, e versus f) and not to a lower stroma content. Higher magnification revealed that wild-type tumor cells typically expressed apical cytokeratin and basal vimentin intermediate filaments (Fig. 4A, g). This coexistence of epithelial and mesenchymal traits is characteristic of a metastable state in between the epithelial and mesenchymal extremes (31). In contrast, the vast majority of mutant tumor epithelium was constituted of vimentin-negative cells, which stained homogeneously for cytokeratin and EpCAM, indicative of a more epithelial state (Fig. 4A, h).

To investigate to what extent stem cell marker expression might coincide with this metastable cell state, expression of Sox6, the only differentially expressed Lgr5-associated marker amenable to immunohistochemistry, was visualized. In wild-type tumors, Sox6 expression was confined to areas of strongest vimentin staining, whereas it was hardly detectable in mutant tumors (Fig. 4B, a versus b).

EMT occurs during development and marks a key step in tumor progression toward metastasis (33). An initial step during EMT, when epithelial cells acquire mesenchymal traits and become more motile, is the breakdown of the basement membrane (35). Immunohistochemical staining of the basement membrane component laminin in wild-type and *Bcl9/Bcl9l*–mutant colon tumors was consistent with the EMT state of wild-type tumors. Thus, virtually no basement membrane laminin was observed in vimentin-positive wild-type tumor epithelium (Fig. 4B, c). In contrast, the epithelium in *Bcl9*$^{-/-}$/*Bcl9l*$^{-/-}$ tumors seemed to be aligned on a contiguous intact laminin membrane (Fig. 4B, d). Concordant observations were made with immunohistochemical staining of collagen IV (data not shown).

Recently, the Prox1 homeobox transcription factor was associated with the acquisition of malignant traits in a similar mouse colon carcinoma model and shown to be directly regulated by β-catenin/Tcf signaling in colorectal cancer (26). The marked difference in Prox1 expression between wild-type and *Bcl9*$^{-/-}$/*Bcl9l*$^{-/-}$ adenocarcinomas (Fig. 3C) was confirmed by immunohistochemical staining (Fig. 4B, e versus f), showing that Prox1 protein expression was largely confined to vimentin-expressing cells and, like vimentin, was expressed only in rare small foci of mutant epithelium (Fig. 4B, g versus h). It is noteworthy that this concomitant expression of vimentin and Prox1 could be observed already in small wild-type tumor lesions but was barely discernible in similar-stage lesions of mutant mice (Supplementary Fig. S3).

Collectively, these findings show that in this tumor model, Bcl9/Bcl9l control a subset of direct Wnt target genes that are involved in the regulation of EMT and stem cell traits.

Discussion

In *Drosophila*, Lgs loss-of-function alleles resulted in phenotypes characteristic of reduced Wnt pathway activity (3). In the mouse, within the context of the adult intestinal epithelium, ablating the Lgs homologues Bcl9/Bcl9l did not cause anomalies reminiscent of other mouse Wnt pathway mutants, which typically resulted in reduced epithelial proliferation and loss of crypts (36–39). Analysis of *Bcl9/Bcl9l*–mutant colon epithelial cells, however, revealed a marked reduction of markers associated with intestinal stem cells and regulated in part by Wnt signaling (ref. 22; Fig. 1A). The absence of any noticeable effect on epithelial homeostasis, the unaltered expression of the stem cell specifying transcription factor Ascl2 (ref. 22; Supplementary Fig. S4), and the similar incidence of chemically induced colon adenocarcinomas (Fig. 2A), which are likely derived from crypt stem cells (40), suggested that specification of intestinal stem cells was largely unaltered in the absence of Bcl9/Bcl9l. The reduced expression of stem cell markers associated with the regenerative deficiency observed in an ulcerative colitis model (Fig. 1) suggested, however, that their function was impaired.

A relationship between Bcl9/Bcl9l and Wnt-mediated regulation of stem cell traits was further revealed when Wnt target gene expression was comprehensively assessed in a mouse chemical carcinogenesis model of colon

Figure 3. Comparative gene expression profiling in chemically induced wild-type versus *Bcl9/Bcl9l*–mutant adenocarcinomas. A, unsupervised hierarchical clustering of gene expression profiles from microdissected tumor epithelium of five randomly chosen tumors (two wild-type and three *Bcl9/Bcl9l*–mutant mice) using all gene probe sets. The dendrogram shows a clear separation of the two genotypes. B, unsupervised hierarchichal clustering using a set of direct Wnt target genes (n = 24), genes involved in EMT (n = 13), and genes with ≥2-fold enriched expression in Lgr5-positive stem cells isolated from the small intestine (n = 50, ref. 22). WT, wild-type mice; KO, *vil-Cre-Bcl9*$^{-/-}$/*Bcl9l*$^{-/-}$ mice. Heat maps indicate relative differences between single samples and average expression (log 2 scale). DBI, Davies-Bouldin index for intercluster separation (17). Sets of Wnt-, EMT-, and intestinal stem cell–related genes were compared with sets of the same size containing the genes with the highest variation across all samples (DBI in square brackets). A lower DBI value indicates a better intercluster separation (see Materials and Methods). C, expression of Wnt target genes listed in B assessed by qRT-PCR (n = 5 ± SE; $P \leq 0.05$, except for *, $P > 0.05$); expression of EMT-related genes listed in B assessed by qRT-PCR (n = 5 ± SE; $P \leq 0.05$, except for *, $P > 0.05$); expression assessed by qRT-PCR of genes contained within the set enriched ≥2-fold in Lgr5-positive intestinal stem cells (22). For intestinal stem cell–related genes, only genes with significantly reduced expression in *Bcl9*$^{-/-}$/*Bcl9l*$^{-/-}$ compared with wild-type tumors are shown (n = 5 ± SE; $P \leq 0.05$). qRT-PCR validations were carried out with cDNA from the same tumor sections as in B.

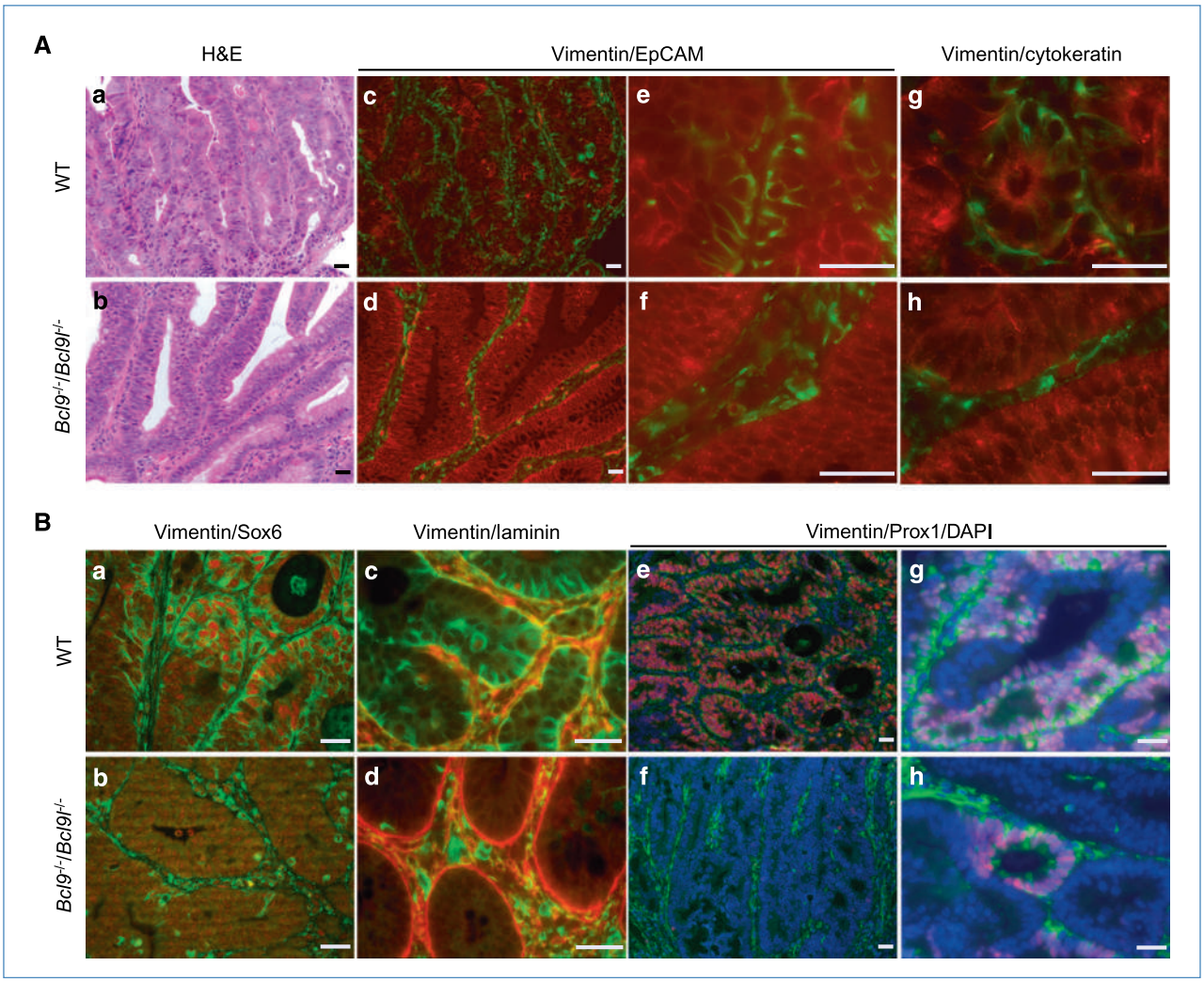

Figure 4. Bcl9/Bcl9l are critical for maintaining colon adenocarcinoma cells in a metastable state characterized by coexpression of epithelial and mesenchymal traits. A, H&E (a, b) and double immunofluorescence staining of wild-type and *Bcl9*$^{-/-}$/*Bcl9l*$^{-/-}$ colon tumors for vimentin/EpCAM (green/red; c, d, e, f) and vimentin/cytokeratin (green/red; g, h). B, immunofluorescence staining of wild-type and *Bcl9*$^{-/-}$/*Bcl9l*$^{-/-}$ colon tumors for vimentin/Sox6 (green/red; a, b), vimentin/laminin (green/red; c, d), and vimentin/Prox1 [green/red; DNA was stained with 4′,6-diamidino-2-phenylindole (DAPI; blue fluorescence); e, f, g, h]. Bar, 25 μm. Histologic analyses were carried out on a set of wild-type and *vil-Cre-Bcl9*$^{-/-}$/*Bcl9l*$^{-/-}$ colon tumors different from those used in Fig. 3.

adenocarcinoma. Transcriptional profiles analyzed with a set of direct Wnt target genes unequivocally distinguished wild-type and *Bcl9/Bcl9l*–mutant tumors. However, the highly significant intercluster separation proved to be due to the downregulation of only some direct Wnt target genes in *Bcl9/Bcl9l*–mutant tumors (Fig. 3B). This subset contained genes that are associated with a mesenchymal phenotype [*T* (*brachyury*; ref. 30); *vimentin* (31)], intestinal stem cells (*Lgr5*; ref. 21), or colon cancer progression (*Prox1*; ref. 26). In addition to Wnt-regulated mesenchymal markers, the expression of genes characteristic of EMT, including *Foxc2*, which promotes mesenchymal differentiation during EMT (41), *Hmga2*, which regulates expression of Snai1 (42), and other EMT transcription factors including Snai2, Twist1, Zeb1/2, as well as the matrix glycoprotein fibronectin, was downregulated in mutant tumors (Fig. 3C). EMT has recently been associated with the generation of cancer cells with stem cell–like properties (34, 43). Strikingly, like in colon epithelium, a gene signature associated with Lgr5-positive intestinal stem cells (22) was strongly attenuated in *Bcl9/Bcl9l*–mutant tumors and clearly distinguished wild-type from *Bcl9/Bcl9l*–mutant tumors (Fig. 3B). Collectively, these observations indicated that Bcl9/Bcl9l are critical for regulating a subset of Wnt target genes relevant to controlling EMT- and stem cell–associated traits. In contrast, Wnt-mediated transduction of proliferative signals remained by and large unaffected by the lack of Bcl9/Bcl9l.

In *Drosophila*, Lgs (Bcl9/Bcl9l) acts as a linker to recruit Pygo to the Arm (β-catenin) complex (3). Pygo is an essential transcriptional coactivator of this complex and has been suggested to exert its function through binding to histone H3 tails and histone decoding (44). Recently, Pygo2 has been

reported to control Wnt signaling–dependent expansion of mouse mammary progenitor cells (45). These findings are in line with our observations and suggest a more general role for Bcl9/Bcl9l and Pygo proteins in regulating stem cell–relevant Wnt target gene expression, possibly by maintaining chromatin in a permissive state (2).

Our observations on the role of Bcl9/Bcl9l may prove clinically relevant. EMT is implicated in tumor invasion and metastasis (33). There is growing evidence suggesting that certain chemotherapy-resistant tumor cells display EMT traits and stem cell properties (32, 46–48). In addition to the lack of EMT features and the loss of stem cell–like properties, *Bcl9/Bcl9l*–mutant tumors showed reduced expression of Wnt-regulated genes that have been directly associated with malignant tumor traits. Thus, Prox1 has been implicated in malignant progression of colon adenocarcinoma, and deletion of *Prox1* in intestinal adenomas resulted in phenotypic changes similar to those described herein, such as the preservation of well-organized basement membranes around Prox1-deleted adenomas (26). It is therefore likely that some of the phenotypic changes caused by the loss of Bcl9/Bcl9l may be due to the downregulation of Prox1. Two other Bcl9/Bcl9l–dependent, direct Wnt target genes, *Fascin1* (29), a key component of filopodia, and *Lef1* (49), have been associated with tumor invasion and metastasis in colon or lung cancer. Expression of Bambi, a newly described Wnt-regulated and Bcl9l-dependent transforming growth factor-β inhibitor, predictive of metastatic potential (50), also proved significantly downregulated in *Bcl9/Bcl9l*–mutant versus wild-type adenocarcinomas (33.6% of mRNA expression in wild-type tumors; $n = 5$; $P = 0.015$). The colon adenocarcinoma model explored herein did not allow assessment of tumor invasiveness and dissemination due to locally advanced growth and precocious intestinal obstruction. Recently, however, RNA interference–mediated silencing of Bcl9 expression in a colon cancer cell line was reported to significantly reduce its metastatic potential (9). Collectively, the virtual abrogation in the absence of Bcl9/Bcl9l of numerous traits associated with malignant tumor progression strongly suggests that targeting Bcl9/Bcl9l function in colon cancers may result in attenuated malignancy, through reduction of their propensity to disseminate and through inhibition of stem cell–associated features, which may restore responsiveness to therapy (32).

These first time observations in loss-of-function mouse mutants indicate that Bcl9/Bcl9l control a subset of Wnt-regulated genes implicated in stem cell control. They warrant further studies to investigate underlying mechanisms involved in selective Wnt target gene regulation as well as to explore the Bcl9/Bcl9l–regulated Wnt subprogram with a view to therapeutically target stem cell–like traits in colon and other Wnt-activated cancers.

Disclosure of Potential Conflicts of Interest

No potential conflicts of interest were disclosed.

Acknowledgments

We thank Drs. Sui Huang (Institute for Biocomplexity and Informatics and Department of Biological Sciences, University of Calgary, Calgary, Alberta, Canada), Roland Sahli (Institute of Microbiology, Centre Hospitalier Unversitaire Vaudois, University of Lausanne, Lausanne, Switzerland), Ivan Stamenkovic (Division of Experimental Pathology, Institute of Pathology, University of Lausanne, Lausanne, Switzerland), Tatiana Petrova (Division of Experimental Oncology, Faculty of Biology and Medicine, University of Lausanne, Lausanne, Switzerland), and Fred Bosman for helpful discussions and advice; Dr. Friedrich Beermann (Swiss Institute for Experimental Cancer Research, Ecole Polytechnique Federale de Lausanne, School of Life Sciences, Lausanne, Switzerland) for blastocyst injections; Drs. Fatima El Marjou (Compartimentation et dynamique cellulaires, Institut Curie, Paris cedex 05, France) and Daniel Louvard (Compartimentation et dynamique cellulaires, Institut Curie, Paris cedex 05, France) for providing *villin-Cre* transgenic mouse strains; Mai Perroud (Department of Biochemistry, University of Lausanne, Lausanne, Switzerland) and Séverine Beck (Swiss Institute for Experimental Cancer Research, School of Life Sciences, Ecole Polytechnique Fédérale de Lausanne, Lausanne, Switzerland) for genotyping; and Gisèle Ferrand and her team (Swiss Institute for Experimental Cancer Research, School of Life Sciences, Ecole Polytechnique Fédérale de Lausanne, Lausanne, Switzerland) and her team for mouse husbandry.

Grant Support

The Swiss National Science Foundation, the Swiss National Center of Competence in Research (NCCR) in Molecular Oncology, and the ISREC Foundation.

The costs of publication of this article were defrayed in part by the payment of page charges. This article must therefore be hereby marked *advertisement* in accordance with 18 U.S.C. Section 1734 solely to indicate this fact.

Received 01/14/2010; revised 06/15/2010; accepted 06/16/2010; published OnlineFirst 08/03/2010.

References

1. Clevers H. Wnt/β-catenin signaling in development and disease. Cell 2006;127:469–80.
2. Mosimann C, Hausmann G, Basler K. β-Catenin hits chromatin: regulation of Wnt target gene activation. Nat Rev Mol Cell Biol 2009;10:276–86.
3. Kramps T, Peter O, Brunner E, et al. Wnt/wingless signaling requires BCL9/legless-mediated recruitment of pygopus to the nuclear β-catenin-TCF complex. Cell 2002;109:47–60.
4. Hoffmans R, Basler K. BCL9-2 binds Arm/β-catenin in a Tyr142-independent manner and requires Pygopus for its function in Wg/Wnt signaling. Mech Dev 2007;124:59–67.
5. Brembeck FH, Schwarz-Romond T, Bakkers J, Wilhelm S, Hammerschmidt M, Birchmeier W. Essential role of BCL9-2 in the switch between β-catenin's adhesive and transcriptional functions. Genes Dev 2004;18:2225–30.
6. de la Roche M, Worm J, Bienz M. The function of BCL9 in Wnt/β-catenin signaling and colorectal cancer cells. BMC Cancer 2008;8:199.
7. Toya H, Oyama T, Ohwada S, et al. Immunohistochemical expression of the β-catenin-interacting protein B9L is associated with histological high nuclear grade and immunohistochemical ErbB2/HER-2 expression in breast cancers. Cancer Sci 2007;98:484–90.
8. Adachi S, Jigami T, Yasui T, et al. Role of a BCL9-related β-catenin-binding protein, B9L, in tumorigenesis induced by aberrant activation of Wnt signaling. Cancer Res 2004;64:8496–501.
9. Mani M, Carrasco DE, Zhang Y, et al. BCL9 promotes tumor progression by conferring enhanced proliferative, metastatic, and angiogenic properties to cancer cells. Cancer Res 2009;69:7577–86.
10. Sakamoto I, Ohwada S, Toya H, et al. Up-regulation of a BCL9-related β-catenin-binding protein, B9L, in different stages of sporadic colorectal adenoma. Cancer Sci 2007;98:83–7.

11. el Marjou F, Janssen KP, Chang BH, et al. Tissue-specific and inducible Cre-mediated recombination in the gut epithelium. Genesis 2004;39:186–93.
12. Reya T, Clevers H. Wnt signalling in stem cells and cancer. Nature 2005;434:843–50.
13. Smyth GK. Linear models and empirical Bayes methods for assessing differential expression in microarray experiments. Stat Appl Genet Mol Biol 2004;3:Article 3.
14. Huang da W, Sherman BT, Lempicki RA. Systematic and integrative analysis of large gene lists using DAVID bioinformatics resources. Nat Protoc 2009;4:44–57.
15. Subramanian A, Tamayo P, Mootha VK, et al. Gene set enrichment analysis: a knowledge-based approach for interpreting genome-wide expression profiles. Proc Natl Acad Sci U S A 2005;102:15545–50.
16. Eisen MB, Spellman PT, Brown PO, Botstein D. Cluster analysis and display of genome-wide expression patterns. Proc Natl Acad Sci U S A 1998;95:14863–8.
17. Davies DL, Bouldin DW. A cluster separation measure. IEEE Trans Pattern Anal Mach Intell 1979;1:224–7.
18. Brembeck FH, Rosario M, Birchmeier W. Balancing cell adhesion and Wnt signaling, the key role of β-catenin. Curr Opin Genet Dev 2006;16:51–9.
19. Lustig B, Jerchow B, Sachs M, et al. Negative feedback loop of Wnt signaling through upregulation of conductin/axin2 in colorectal and liver tumors. Mol Cell Biol 2002;22:1184–93.
20. Ayabe T, Satchell DP, Wilson CL, Parks WC, Selsted ME, Ouellette AJ. Secretion of microbicidal α-defensins by intestinal Paneth cells in response to bacteria. Nat Immunol 2000;1:113–8.
21. Barker N, van Es JH, Kuipers J, et al. Identification of stem cells in small intestine and colon by marker gene Lgr5. Nature 2007;449:1003–7.
22. van der Flier LG, van Gijn ME, Hatzis P, et al. Transcription factor achaete scute-like 2 controls intestinal stem cell fate. Cell 2009;136:903–12.
23. Cooper HS, Murthy SN, Shah RS, Sedergran DJ. Clinicopathologic study of dextran sulfate sodium experimental murine colitis. Lab Invest 1993;69:238–49.
24. Kohno H, Suzuki R, Sugie S, Tanaka T. β-Catenin mutations in a mouse model of inflammation-related colon carcinogenesis induced by 1,2-dimethylhydrazine and dextran sodium sulfate. Cancer Sci 2005;96:69–76.
25. Takahashi M, Fujita M, Furukawa Y, et al. Isolation of a novel human gene, APCDD1, as a direct target of the β-catenin/T-cell factor 4 complex with probable involvement in colorectal carcinogenesis. Cancer Res 2002;62:5651–6.
26. Petrova TV, Nykanen A, Norrmen C, et al. Transcription factor PROX1 induces colon cancer progression by promoting the transition from benign to highly dysplastic phenotype. Cancer Cell 2008;13:407–19.
27. Gilles C, Polette M, Mestdagt M, et al. Transactivation of vimentin by β-catenin in human breast cancer cells. Cancer Res 2003;63:2658–64.
28. Stein U, Arlt F, Walther W, et al. The metastasis-associated gene S100A4 is a novel target of β-catenin/T-cell factor signaling in colon cancer. Gastroenterology 2006;131:1486–500.
29. Vignjevic D, Schoumacher M, Gavert N, et al. Fascin, a novel target of β-catenin-TCF signaling, is expressed at the invasive front of human colon cancer. Cancer Res 2007;67:6844–53.
30. Arnold SJ, Stappert J, Bauer A, Kispert A, Herrmann BG, Kemler R. Brachyury is a target gene of the Wnt/β-catenin signaling pathway. Mech Dev 2000;91:249–58.
31. Lee JM, Dedhar S, Kalluri R, Thompson EW. The epithelial-mesenchymal transition: new insights in signaling, development, and disease. J Cell Biol 2006;172:973–81.
32. Polyak K, Weinberg RA. Transitions between epithelial and mesenchymal states: acquisition of malignant and stem cell traits. Nat Rev Cancer 2009;9:265–73.
33. Thiery JP, Acloque H, Huang RY, Nieto MA. Epithelial-mesenchymal transitions in development and disease. Cell 2009;139:871–90.
34. Mani SA, Guo W, Liao MJ, et al. The epithelial-mesenchymal transition generates cells with properties of stem cells. Cell 2008;133:704–15.
35. Levayer R, Lecuit T. Breaking down EMT. Nat Cell Biol 2008;10:757–9.
36. Fevr T, Robine S, Louvard D, Huelsken J. Wnt/β-catenin is essential for intestinal homeostasis and maintenance of intestinal stem cells. Mol Cell Biol 2007;27:7551–9.
37. Ireland H, Kemp R, Houghton C, et al. Inducible Cre-mediated control of gene expression in the murine gastrointestinal tract: effect of loss of β-catenin. Gastroenterology 2004;126:1236–46.
38. Korinek V, Barker N, Moerer P, et al. Depletion of epithelial stem-cell compartments in the small intestine of mice lacking Tcf-4. Nat Genet 1998;19:379–83.
39. Pinto D, Gregorieff A, Begthel H, Clevers H. Canonical Wnt signals are essential for homeostasis of the intestinal epithelium. Genes Dev 2003;17:1709–13.
40. Barker N, Ridgway RA, van Es JH, et al. Crypt stem cells as the cells-of-origin of intestinal cancer. Nature 2009;457:608–11.
41. Mani SA, Yang J, Brooks M, et al. Mesenchyme Forkhead 1 (FOXC2) plays a key role in metastasis and is associated with aggressive basal-like breast cancers. Proc Natl Acad Sci U S A 2007;104:10069–74.
42. Thuault S, Tan EJ, Peinado H, Cano A, Heldin CH, Moustakas A. HMGA2 and Smads co-regulate SNAIL1 expression during induction of epithelial-to-mesenchymal transition. J Biol Chem 2008;283:33437–46.
43. Morel AP, Lievre M, Thomas C, Hinkal G, Ansieau S, Puisieux A. Generation of breast cancer stem cells through epithelial-mesenchymal transition. PLoS One 2008;3:e2888.
44. Fiedler M, Sanchez-Barrena MJ, Nekrasov M, et al. Decoding of methylated histone H3 tail by the Pygo-BCL9 Wnt signaling complex. Mol Cell 2008;30:507–18.
45. Gu B, Sun P, Yuan Y, et al. Pygo2 expands mammary progenitor cells by facilitating histone H3 K4 methylation. J Cell Biol 2009;185:811–26.
46. Creighton CJ, Li X, Landis M, et al. Residual breast cancers after conventional therapy display mesenchymal as well as tumor-initiating features. Proc Natl Acad Sci U S A 2009;106:13820–5.
47. Gupta PB, Onder TT, Jiang G, et al. Identification of selective inhibitors of cancer stem cells by high-throughput screening. Cell 2009;138:645–59.
48. Yang AD, Fan F, Camp ER, et al. Chronic oxaliplatin resistance induces epithelial-to-mesenchymal transition in colorectal cancer cell lines. Clin Cancer Res 2006;12:4147–53.
49. Nguyen DX, Chiang AC, Zhang XH, et al. WNT/TCF signaling through LEF1 and HOXB9 mediates lung adenocarcinoma metastasis. Cell 2009;138:51–62.
50. Fritzmann J, Morkel M, Besser D, et al. A colorectal cancer expression profile that includes transforming growth factor β inhibitor BAMBI predicts metastatic potential. Gastroenterology 2009;137:165–75.